Metallurgical and Materials Engineering *Research paper*
Association of Metallurgical Engineers of Serbia AMES *https://doi.org/10.30544/627*

DENSITY FUNCTIONAL PREDICTION OF THE STRUCTURAL, ELASTIC, ELECTRONIC, AND THERMODYNAMIC PROPERTIES OF THE CUBIC AND HEXAGONAL (*c*, *h*)-Fe_2Hf

M. Hamici[1], T. Chihi[2], M.A Ghebouli[2], M. Fatmi[2,], B. Ghebouli[3], Sameh I. Ahmed [4]*

[1] Dosage Analysis and Characterization Laboratory (DAC), University Farhet Abbas of Setif 1, 19000, Algeria
[2] Research Unit on Emerging Materials (RUEM), University Farhet Abbas of Setif 1, 19000, Algeria
[3] Laboratory of Studies Surfaces and Interfaces of Solids Materials, Department of Physics, Faculty of Sciences, University Ferhat Abbas of Setif 1, 19000, Algeria
[4] Department of Physics, College of Science, Taif University, P.O. Box 11099, Taif 21944, Saudi Arabia

Received 23.03.2021
Accepted 09.06.2021

Abstract

The structural, elastic, electrical, and thermodynamic characteristics of Fe_2Hf cubic and hexagonal phases with space group Fd-3m and P63/mmc are presented using the generalized gradient approximations. The k-points mesh density and plane-wave energy cut-off accomplish the energy convergence. The computed equilibrium parameters are closer to the theoretical data. The elastic tensor and crystal anisotropy of ultra-incompressible Fe_2Hf are computed in a wide pressure range. The isothermal and adiabatic bulk modulus, as well as the heat capacity of Fe_2Hf is successfully calculated utilizing the quasi-harmonic Debye Model. The Fd-3m and P63/mmc Fe_2Hf structures are stable in the studied pressure range.

Keywords: elastic stability; thermodynamic properties; Fe_2Hf compound.

[*]Corresponding author: M. Fatmi, *fatmimessaoud@yahoo.fr*

Introduction

Fe_2Hf structures have not been produced in crystalline form. We propose the cubic and hexagonal structures. The strength and hardness of materials are determined from elastic constants under pressure. These crucial parameters determine the crystal's reaction to external forces, as defined by the bulk and shear modulus. The elastic characteristics of cubic and hexagonal structures are also obtained. The structural, elastic and thermodynamic parameters of hexagonal Fe_2Hf structure under pressure were treated for the first time. *Koki Ikeda et al*. [1] investigated the structure and magnetism in the iron hafnium system. The conclusion is that hexagonal $MgZn_2$-type Fe_2Hf and cubic $MgCu_2$-type Fe_2Hf exist above 1673 K and below 1273 K. *S. Kobayashi et al.* [2-3] observed periodic arranged rows of fine Fe_2Hf Laves phase particles produced in a 9 % chromium ferritic matrix. *J. Belosevic-Cavor et al.* [4] investigated the magnetic characteristics, Mossbauer Effect, and first-principles computations of Fe_2Hf with a C14 type structure in the laves phase. *Masao Takeyama* [5] discovered the hexagonal lattice for Fe_2Hf with space group P63/mmc (N_0 194). Fe_2Hf has the $MgCu_2$ type C15 cubic structure with a narrow content range around the stoichiometry. It also crystallizes in the $MgZn_2$ (C14) hexagonal structural type. The hexagonal phase appears along the dominant cubic structure. The aim of this work is to present a theoretical investigation of the structural and thermodynamic properties of cubic and hexagonal Fe_2Hf structures. The cubic Fe_2Hf (hexagonal Fe_2Hf) structure has the space group 227, *Fd-3m* and Cu_2Mg-type (194, *P63/mmc* and Zn_2Mg-type). The non-equivalent atoms are Fe (0.625, 0.625, 0.625), Hf (0, 0, 0) and lattice constant a=6.882Å [Fe_1 (0, 0, 0), Fe_2 (0.8, 0.6, 0.25), Hf (1/3, 2/3, 0.06) and lattice parameters a=b= 4.968Å, c=8.098Å] for cubic Fe_2Hf (hexagonal Fe_2Hf).

Computational details

We use CASTEP, PWG and GGA as exchange-correlation potential. Without taking account the spin polarized, we must investigate and examine the convergence of calculated total energies with respect to the plane wave cut-off E_{cut} =380 eV (E_{cut} =385 eV) in the cubic (hexagonal) phase as reported in Fig.1 (a) and (b) respectively.

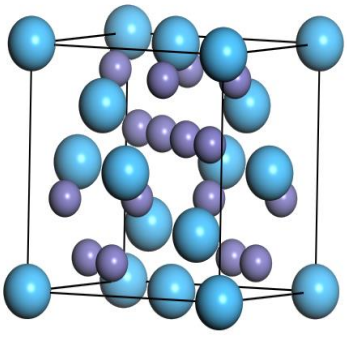

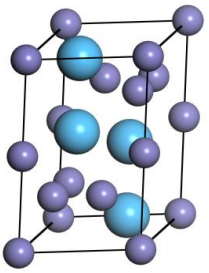

Fig. 1. Unit-cell of Fe_2Hf cubic and hexagonal crystal, the large and small balls represent Hf and Fe atoms, respectively.

Structural properties

We use first-principles computations to investigate the structural, elastic, electrical, and thermodynamic properties of Fe_2Hf with cubic (hexagonal) structure under pressures up to 10 GPa (15GPa). The elastic characteristics of cubic and hexagonal Fe_2Hf under pressure are examined, where the mechanical stability is ensured. The Debye model is used to derive thermodynamic parameters such as heat capacity, thermal expansion and Debye temperature. However, it is difficult to study it experimentally because of the small size and time scale at which the functional properties appeared. Theoretical modeling offers a way to overcome these difficulties through "virtual experiments" that can enable us to explore the phase space. The DFT is widely used in quantum computation in condensed matter physics [6-8]. DFT is a general-purpose computational method, and can be applied to most systems. Although density functional theory is more precise and perfect in theory, it involves various approximations in practice, [9-11], and mesh size for Brillouin zone for plane-wave basis [12-14]. More include plane waves; the better the wave function is modeled. The k-points mesh controls the BZ integration, can play a huge role in the quality of the results and heavily depends on the number of these points on the mesh-grid, especially for metals. The plane wave basis set, in the DFT wave function is expanded in terms of its periodicity and case of use. The DFT wave function is expanded in terms of a plane wave basis set [15]:

$$\psi(r) = \sum_G C_G e^{i(G+K)r} \qquad 1$$

And the cut-off energy E_{cut} is defined as:

$$E_{cut} = \frac{\hbar^2}{2m}|G_{cut}|^2 \qquad 2$$

$$|G + K| < E_{cut} \qquad 3$$

The Fig. 1 represents total energy as a function of k-points. The convergence has been achieved in the k-points sampling of 1x1x1 for total energy convergence tolerance (1.0 10^{-6} eV/atom).

The rest of this paper is structured as follows. The computational method is described in section 2. The results and some discussions of structural, elastic and thermodynamic properties of Fe_2Hf under pressure are presented and compared with available experimental and theoretical data in section 3. The large and small balls of Fe and Hf atoms are shown in Fig. 2. The convergence of calculated number of points is 6x6x6 of *c*-Fe_2Hf and *h*-Fe_2Hf, as shown in Fig.3. We show the plot of energy versus volume for cubic and hexagonal Fe_2Hf in Fig.4 (a) and (b). The calculations of the structural, elastic, and thermodynamic properties were performed using the CASTEP code [16,17]. Fe (3d64 s2) and Hf (4f145 d26 s2) orbitals are considered as valence electrons. The Brillouin zone sampling was done using the Monkhorst-Pack mesh 6x6x6 for cubic and hexagonal structures of Fe_2Hf [18]. The most stable structure requires its optimization using the Broyden-Fletcher-Goldfarb-Shenno (BFGS) minimization technique. Setting self-consistent convergence conditions: total energy per atom was less than 0.2 eV, force per atom was less than 0.05 eV, offset tolerance was less than 0.0002 A, and stress bias was less than 0.1GPa. It should be noted that the predicted total energies of cubic and hexagonal (c- h)- Fe_2Hf structures have negative values, indicating an exothermic reaction, as shown in Table 1. According to the total energies, hexagonal structure is more stable than cubic structure.

Table 1. The calculated lattice constant (Å), volumes ($Å^3$), bulk modulus, elastic constants, shear modulus, Young's modulus, B/G ratio, density, sound velocities, and Debye temperature for (c- h)- Fe_2Hf structures.

	Cubic structure	Hexagonal structure
Cuttofenegy (eV)	380	385
KxKxK	6x6x6	6x6x6
Total energy (eV)	-4280.10	-8560.42
a(Å)	4.883	4.858 (4.968)
b(Å)	4.883	4.858(4.968)
c(Å)	4.883	8.042(8.098)
Volume ($Å^3$)	82.340	164.456
Z	2	1
B(GPa)	218.90	222.496
C_{11}	316.256	358.613
C_{12}	170.230	180.066
C_{44}	96.075	91.652
C_{33}	-	347.149
C_{13}	-	146.081
C_s	86.075	93.721
ρ	11.0766	11.7201
v_l(m/s)	5488.5230	5447,6170
v_t(m/s)	2787.6312	2827,834
v_m(m/s)	3123.573	3164,9355
Θ_D (K)	378	394
Y	230.119	246.595
ν	0.32479	0.31557

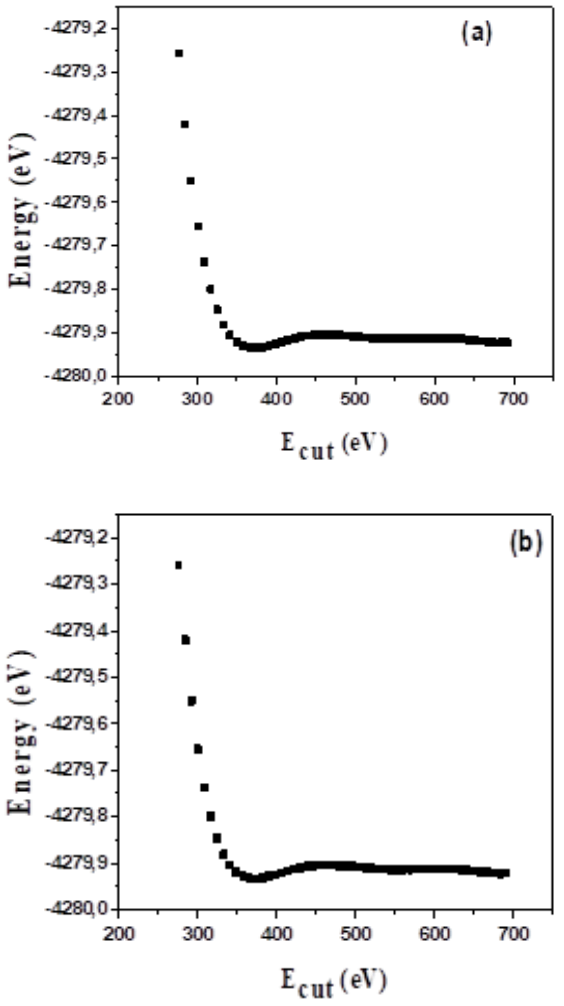

Fig. 2. Energy versus E_{cut} in cubic (a) and hexagonal (b) structure.

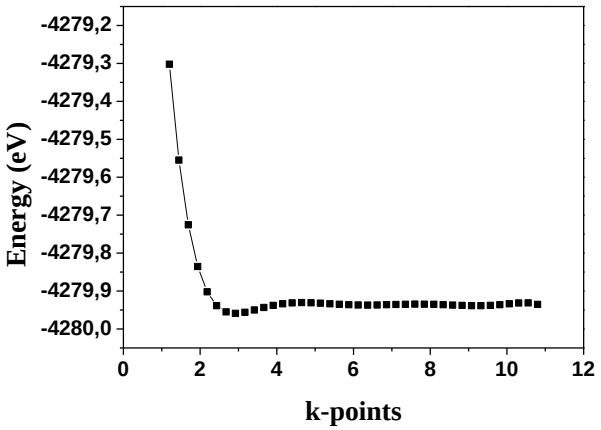

Fig. 3. Energy versus number of k points of our computed compounds.

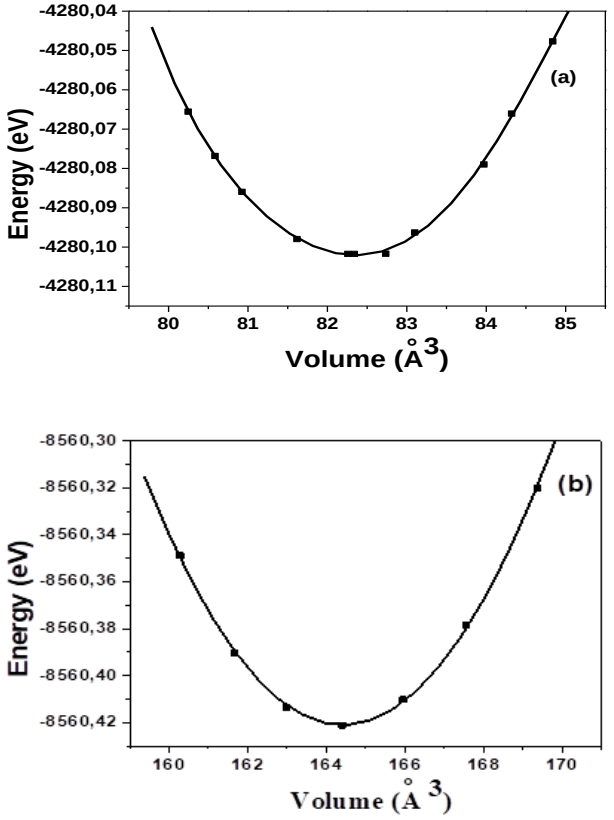

Fig. 4. Energy versus volume for Fe_2Hf in cubic (a) and hexagonal (b) structure.

Elastic constants

The elastic constants for the system are established using a Taylor series expansion of the total energy, E (V), in comparison to a modest deformation δ of the lattice unit cell volume V. The energy of system limitation is expressed as follow [19]:

$$E(V,\delta) = E(V_0,0) + V_0[\sum_i \tau_i \xi_i \delta_i + \frac{1}{2}\sum_{ij} C_{ij}\delta_i \xi_i \delta_j] \quad 4$$

Where $E(V_0, 0)$ is the energy of an unstrained system with V_0, is a stress tensor element, and is a factor to account for the Voigt index. Asymmetric and isotropic materials have between 21 and 2 independent elastic constants, while cubic and hexagonal crystals have 3 and 5 independent elastic constants, respectively. C_{11}, C_{44}, and C_{12} for cubic crystals and C_{11}, C_{33}, C_{44}, C_{12}, and C_{13} for hexagonal crystals are the three independent elastic constants. The first-order and second-order derivatives of the potential are well-known for giving forces and elastic constants. As a result, checking the accuracy of the calculations for forces and elastic constants is critical. Let us recall that the effect of pressure on elastic constants is critical for understanding interatomic interactions, mechanical stability, and phase transition mechanisms, at the very least. For cubic and hexagonal Fe_2Hf structures, the relevant bulk moduli are found as a function of pressure up to 50 GPa. When pressure is increased as shown in Fig. 5, all elastic constants, as well as bulk moduli B, increase linearly.

$$B = (C_{11} + 2C_{12})/3 \quad 5$$

The bulk modulus value estimated using the second approach agrees with the bulk modulus calculated using the first method. The generalized elastic stability criterion for Fe_2Hf in a cubic crystal is as follows:

$$(C_{11} + 2C_{12})/3 > 0 \qquad C_{44} > 0 \quad 6$$

$$(C_{11} - C_{12})/2 > 0 \quad 7$$

For Fe_2Hf in a hexagonal crystal, the elastic stability criteria [20,21] are:

$$C_{11} > 0, C_{33} > 0,\ C_{44} > 0,\ C_{66} > 0\ , C_{11} - C_{12} > 0, C_{11} + C_{33} + C_{12} > 0, (C_{11} + C_{12})C_{33} - 2C_{13}^2 > 0 \quad 8$$

The fact that all of the foregoing conditions are violated by the elastic constants of Fe_2Hf in the cubic [hexagonal] crystal suggests that it is instable [stable]. The shear anisotropy factors A(Cij)=0.88 and kc/ka = 1.22 for Fe_2Hf with hexagonal structure, the B and G for hexagonal structures are calculated as follows [22,23]:

$$B = \frac{2}{9}\left(C_{11} + C_{12} + 2C_{13} + \frac{1}{2}C_{33}\right) \quad 9$$

$$G = \left\{C_{44}[C_{44}(C_{11} - C_{12})/2]^{1/2}\right\}^{1/2} \quad 10$$

$$E = \frac{[C_{33}(C_{11}+C_{12})-2C_{13}^2](C_{11}-C_{12})}{C_{11}C_{33}-C_{13}^2} \quad 11$$

$$A = \frac{2C_{44}}{C_{11}-C_{12}} \quad 12$$

$$\nu = \frac{C_{12}C_{33}-C_{13}^2}{C_{11}C_{33}-C_{13}^2} \quad 13$$

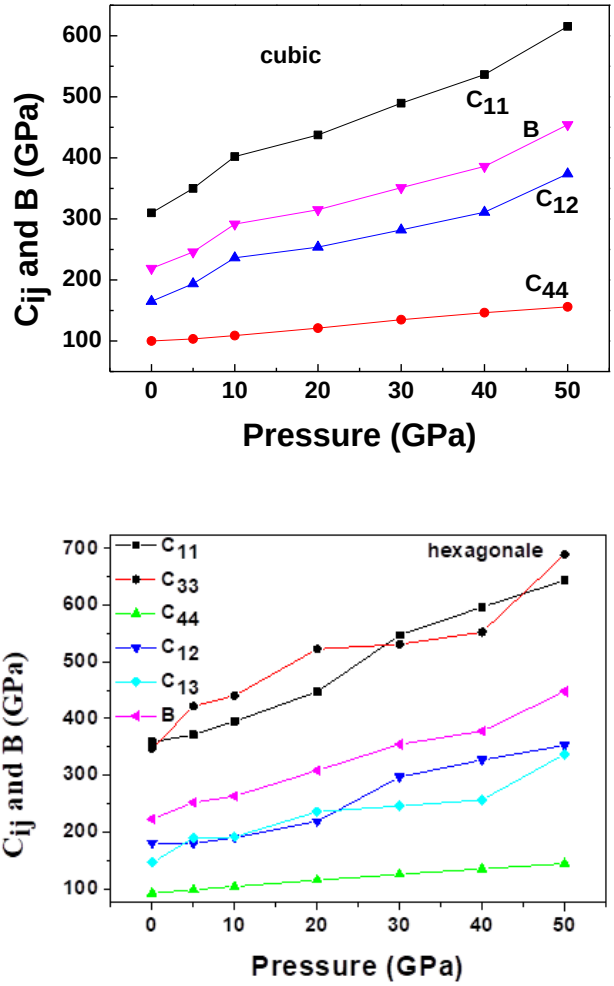

Fig. 5. The elastic constants of the cubic and hexagonal structures of Fe_2Hf compound under pressure up to 50 GPa at 0 K.

We can conclude that the bulk modulus is 219 GPa for cubic Fe_2Hf and 222 GPa for hexagonal one. All values are exceptionally high, exceeding or matching other hard materials, including boron carbide (B_4C, 200 GPa), silicon carbide (SiC, 248 GPa),

sapphire (Al_2O_3, 252 GPa), and cubic boron nitride (*c*-BN, 367 GPa) [24]. Pugh [25] proposed the B/G ratio to represent a measure of a "machine able behavior". A high B/G value (2.444 for hexagonal Fe_2Hf type structure) is linked to ductility, while a low one is linked to brittleness. Around 1.75 is the crucial number that distinguishes between ductile and brittle behavior. Diamond, for example, has a B/G of 0.80 [26], whereas aluminum, cobalt, rhodium, and iridium, respectively, have B/G ratios of 2.74, 2.43, 1.77, and 1.74. We find a B/G estimated ratio of 2.44 for the hexagonal structure of Fe_2Hf combination. Due to the fact that Fe_2Hf compounds are ductile; furthermore, the elastic constants data ($C_{11} - C_{12} > 0$) can be used to forecast the hexagonal structure's mechanical stability at 0 GPa. The elastic constants of pure Fe_2Hf are reported in Table 1. The average sound velocity V_m [26,27] can be used to calculate the Debye temperature.

$$V_m = \left[\frac{1}{3} \left(\frac{2}{V_s^3} + \frac{1}{V_l^3} \right) \right]^{-1/3} \qquad 14$$

The shear and longitudinal sound velocities are V_s and V_l.
In Table 1, the longitudinal, transverse, and average sound velocities, as well as the Debye temperature of Fe_2Hf have been determined. We have estimated the sound velocities and Debye temperature for the Fe_2Hf compounds from our elastic constants at 0GPa and 0K. The experimental and estimated sound velocities and Debye temperatures are comparable.

Electronic structure

The electronic characteristics of Fe_2Hf are studied in this section. At equilibrium lattice constants; Fig. 6 displays the (DOS) for our compound configurations. Only the Fermi energy level's vicinity is shown here. Except for a few changes, the DOS profiles of Fe_2Hf are identical throughout the energy range. Near the Fermi level, the DOS is primarily derived from the M-d bands M (Fe_2Hf) in cubic and hexagonal structures, implying that our compounds are all conductive and that the transition metal's d bands play a dominant role in electrical transport. This phenomenon is particularly pronounced in hexagonal structures. In cubic and hexagonal Fe_2Hf, the DOS at the Fermi level $n(E_F)$ is predicted to be 10.69 states/eV unit cell for cubic Fe_2Hf and 20.11 eV for hexagonal Fe_2Hf, suggesting the metallic material.

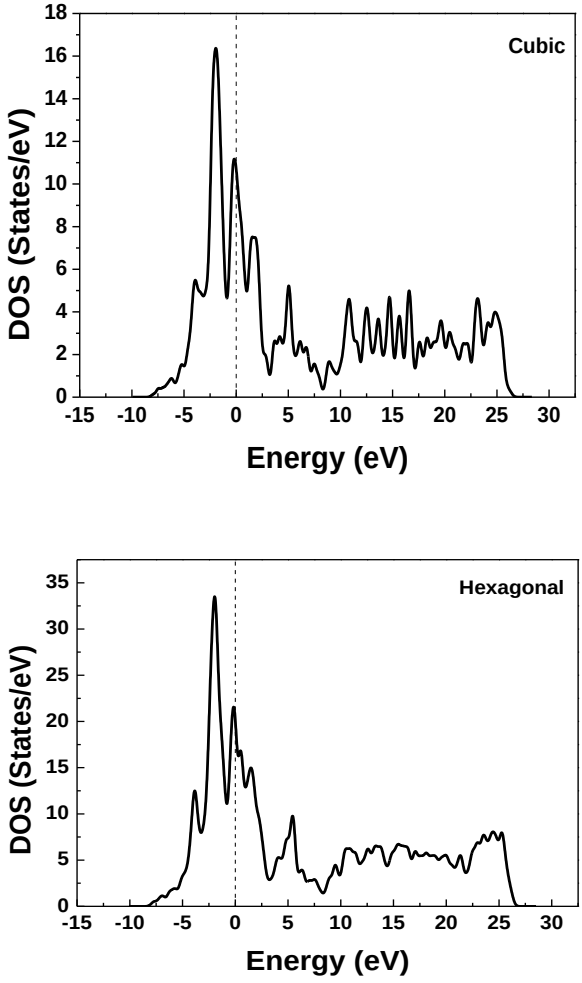

Fig. 6. The total electronic density of state for Fe_2Hf in cubic and hexagonal structures.

Thermodynamic properties

A study of the effects of chemistry and crystal structure must be performed for motors with operating temperatures in the region of 2000°C that will require materials that can withstand. Intermetallic compounds with high melting temperatures are candidates for these applications. Thermodynamics is mainly based on temperature and entropy, which is the degree of disorganization of the material. Physical properties under pressures and temperatures have important meanings to accelerate the understanding and synthesis of (*c*, *h*)- Fe_2Hf structures. The investigation of the thermal capacity of crystals is an interesting subject in solid state physics because it enters many applications, and provides essential information on its vibratory properties. According

to the standard theory of elastic continuum, two limiting cases are correctly predicted. At sufficiently low temperatures, the thermal capacity C_V is proportional to T^3. At high temperature, C_V tends to the limit Petit and Dulong. Applying the quasi-harmonic Debye model to the (*c*, *h*)- Fe_2Hf structures, we calculated the thermal capacity C_V, and the Debye temperature Θ at different temperatures. Now we investigate the dependences of bulk modulus B on temperature T and pressure P. B is plotted in Fig. 7.

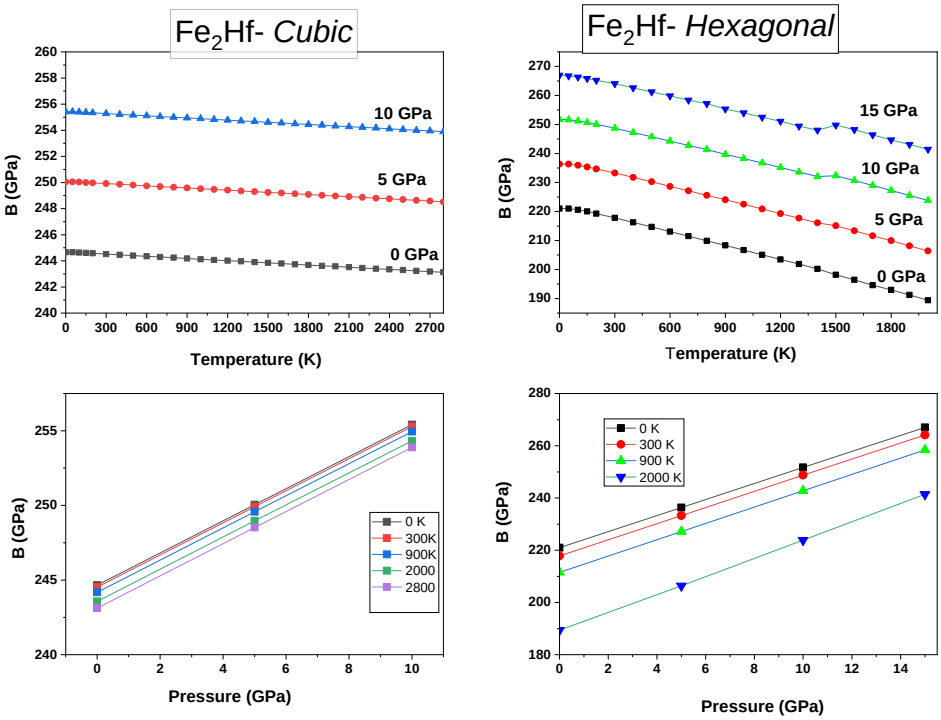

Fig. 7. Variation of bulk modulus with temperature T and pressures for c- Fe_2Hf and h- Fe_2Hf (upper panel) respectively.

The bulk modulus *B* decreases with increasing temperature T in a quasi-linear manner for both *c*- Fe_2Hf and *h*- Fe_2Hf structures. The calculated B_0 at (T=0 K) is 244.5 GPa for *c*- Fe_2Hf and 222 GPa for *h*- Fe_2Hf structures. We can see that the *B* decreases [increases] with temperature (upper panel) [P] [lower panel] at a given pressure [T] for both *c*- Fe_2Hf (slowly decreases) and *h*- Fe_2Hf structures. The resulting Debye temperature Θ versus temperature [P] (upper panel) [lower panel] for *c*- Fe_2Hf and *h*- Fe_2Hf structures is shown in Fig. 8.

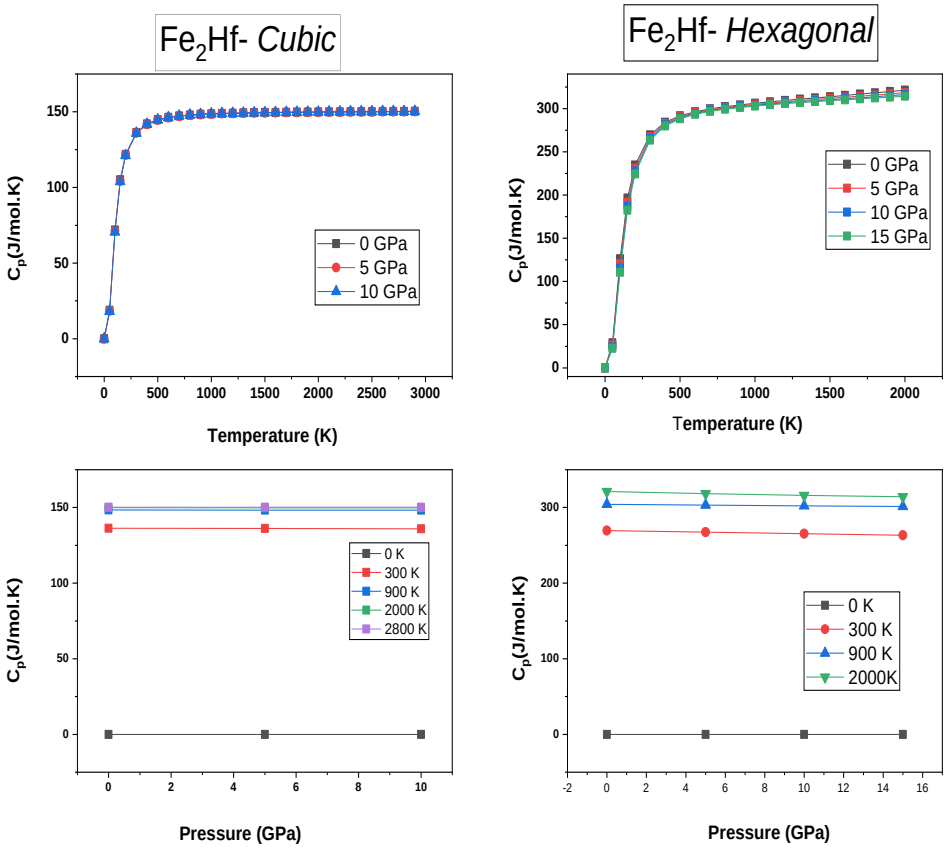

Fig. 8. Variation of constant pressure heat capacity C_P with temperature T and pressures for c- Fe_2Hf and h- Fe_2Hf (upper panel) respectively.

From the quasi-harmonic Debye model, we obtained the Debye temperature Θ = 415.5 K and 458 K at P=0 GPa and T=0 K for *c*- Fe_2Hf and *h*- Fe_2Hf structures Fig. 9. The heat capacity C_P and C_V, represents the heat absorbed by the crystal at constant pressure or constant volume necessary to raise the temperature of one mole of a pure substance by one degree K generated by this transformation. The heat capacity of a crystal is given by a relation deduced from the vibratory motions of the crystal lattice it is also mandatory for many applications. For solids and liquids, the variation of the PV product with the temperature is negligible. Consequently, in the condensed phase, the volume and constant pressure heat capacities have similar values $C_P \sim C_V$ for both *c*- Fe_2Hf and *h*- Fe_2Hf structures.

In Fig. 10, we see the sharp increase of C_P and C_V from 0 to 500 K. At high temperature, the C_P and C_V tends to a constant value (300 $J.mol^{-1}K^{-1}$) [150 $J.mol^{-1}K^{-1}$] for (*c*- *h*)- Fe_2Hf the so-called Dulong-Petit limit of $3nk_B$ value [**30**]. We can conclude that the volume heat capacity in 300°K is in the range of 120- 150 $J.mol^{-1}K^{-1}$ for *c*- Fe_2Hf and 250- 300 $J.mol^{-1}K^{-1}$for *h*- Fe_2Hf. All of the values in this range are extremely high, surpassing or equal those of other hard materials, including silicon oxide (SiO_2, 71.5

J.mol^{-1}K^{-1}), sapphire (Al_2O_3, 120.5 J.mol^{-1}K^{-1}), and (Cr_2O_3, 125.1 J.mol^{-1}K^{-1}) and approaching that of diamond (B_0 = 442 GPa).The volume expansion coefficient α_0f (*c*, *h*)-Fe_2Hf structures as function of T (upper panel) and P (lower panel) is plotted in Fig. 11. At 0 GPa and 300 K, $\alpha = 0.41242 \times 10^{-5}$ K^{-1} for *c*-Fe_2Hf and 0.42234×10^{-5} K^{-1} for *h*-Fe_2Hf. It is shown that, for a given P [T], α increases [constant] with T [P], especially at 0 GPa and gradually tends to a linear increase at high T, for *c*- Fe_2Hf and slightly different for *h*- Fe_2Hf structures. We show in Fig. 12, the entropy function of the temperature at different pressures and of the pressure at different temperatures of the two types of c-FeHf and h-Fe2Hf structures of the compound. We show that the entropy increase parabolically with increasing temperature. We notice that these curves have the same shape except the existence of q slight offset at high temperature for the case of the hexagonal type (upper panel).

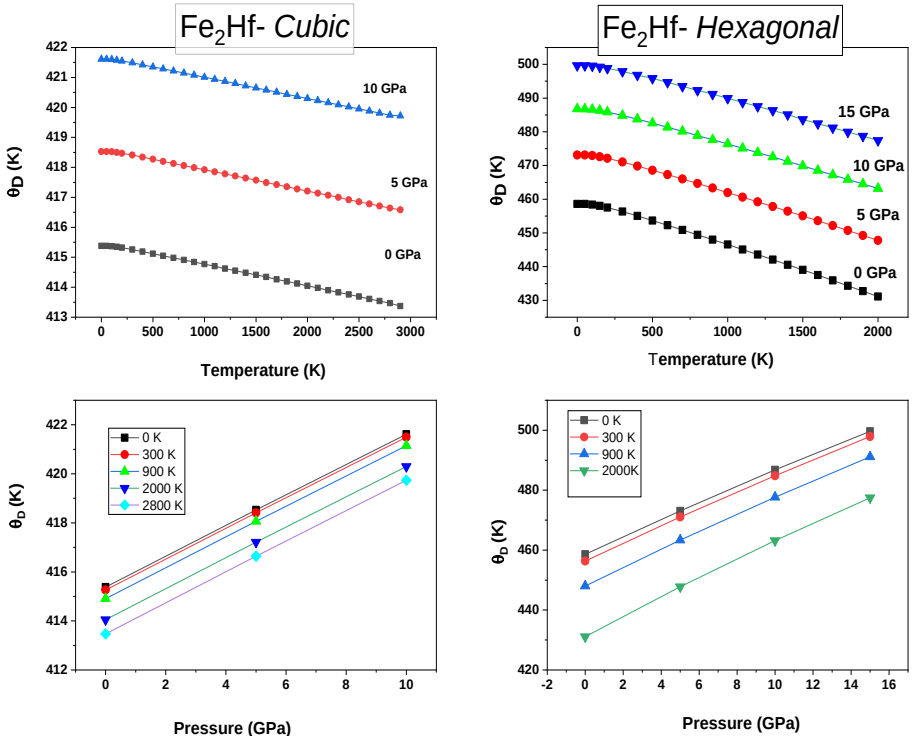

Fig. 9. Variation of Debye temperature with temperature T and pressures for c- Fe_2Hf and h- Fe_2Hf (upper panel), respectively.

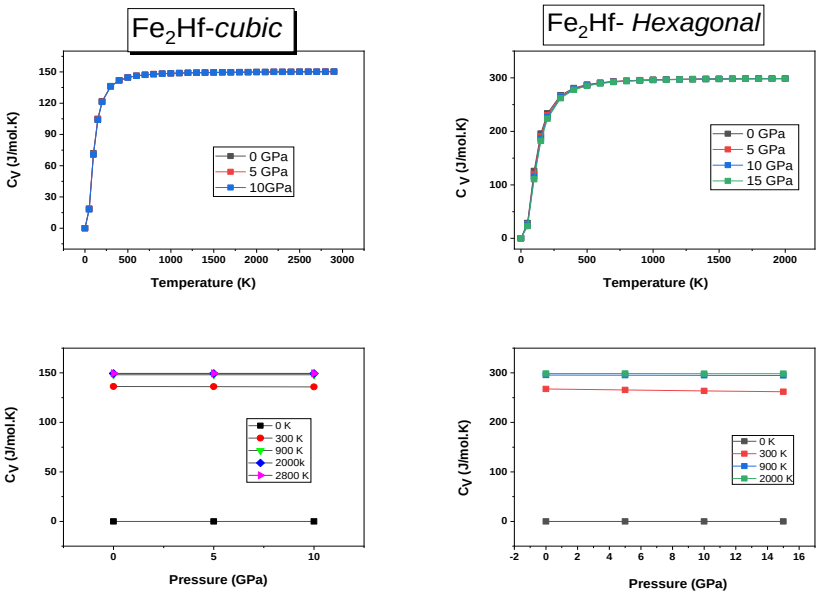

Fig. 10. Variation of constant volume heat capacity C_V with temperature T and pressures for c- Fe_2Hf and h- Fe_2Hf (upper panel), respectively.

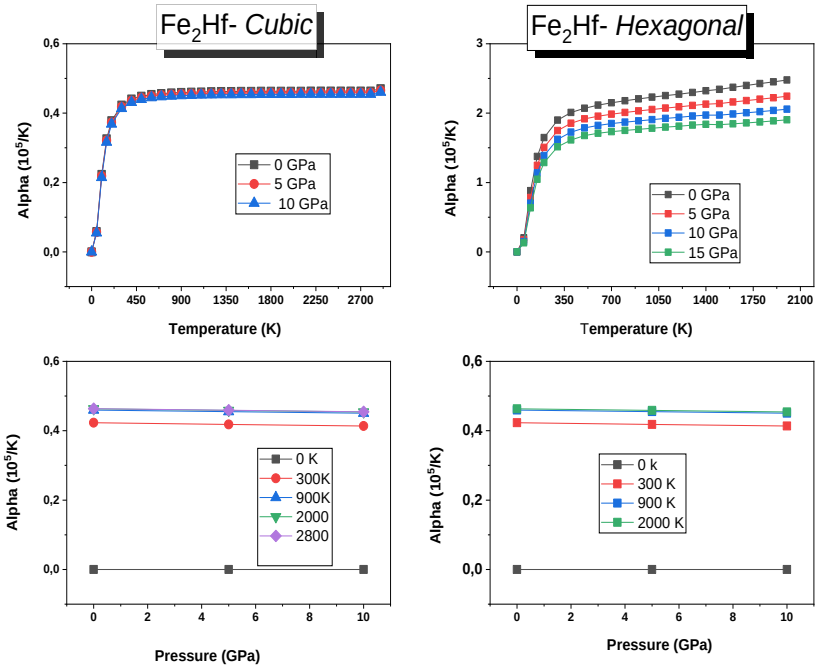

Fig. 11. Variation of volume expansion coefficient α with temperature T and pressures for c- Fe_2Hf and h- Fe_2Hf (upper panel), respectively.

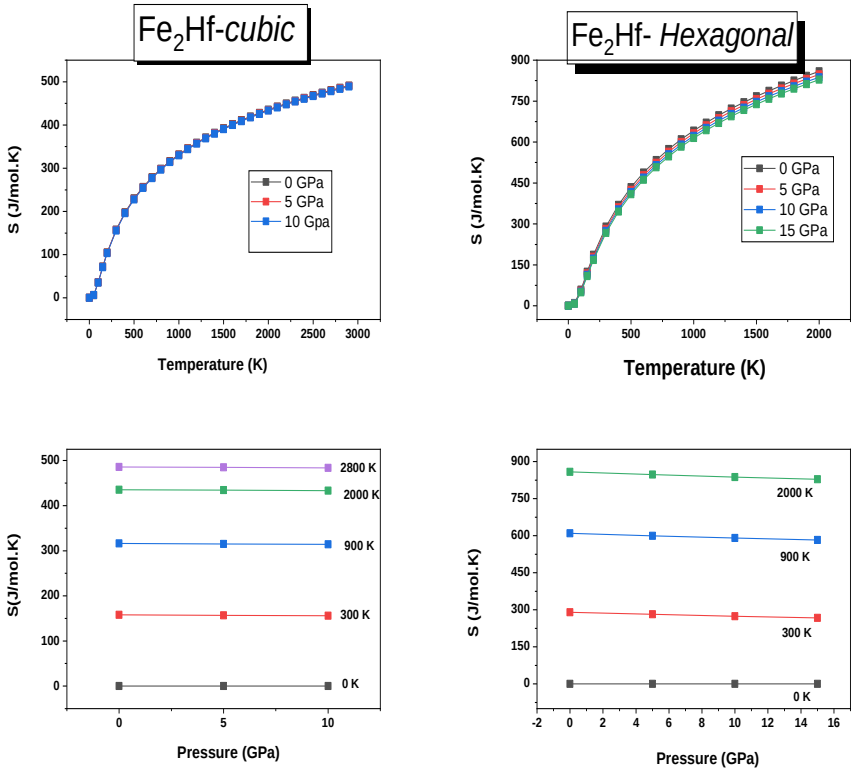

Fig. 12. Variation of entropy S with temperature T and pressures for c- Fe_2Hf and h- Fe_2Hf (upper panel), respectively.

Conclusion

We draw theoretical findings for structural, elastic, mechanical, electrical, and thermodynamic properties of Fe2Hf in the cubic and hexagonal solid phases based on ab initio total energy calculations. The lattice constants obtained are fairly close to the experimental values. Hexagonal structures are more stable than cubic structures in terms of total energy. The DOS at the Fermi level n(EF) for cubic is 10.69 states/eV unit cell, while the DOS for hexagonal is 20.11 states/eV, indicating metallic material. In general, the molecule with a lower n(EF) is more stable. As a result, the total energy minimum values and the values generated from the total energy minimum agree well. All estimated bulk modulus values are exceptionally high, exceeding or equaling those of other hard materials such as boron carbide (B4C, 200 GPa), silicon carbide (SiC, 248 GPa), sapphire (Al2O3, 252 GPa), and cubic boron nitride (CBN, 252 GPa) (c-BN, 367 GPa). For the other estimated qualities in this paper, there are no previous computations or experimental data to compare with.

Acknowledgments

Taif University Research Supporting Project number (TURSP-2020/66), Taif University, Taif, Saudi Arabia.

References

[1] Koki Ikeda: Inter J Mater Research, 68 (1977) 195-198.
[2] S. Kobayashi, K. Kimura, K. Tsuzaki: Intermetallics, 46 (2014) 80-84.
[3] S. Kobayashi, T. Hibaru: ISIJ International, 55 (2015) 293-399.
[4] J. Belosevic-Cavor, V. Koteski, N. Novakovic, G. Concas, F. Congiu, G. Spano: Euro Phys J B, 50 (2006) 425-430.
[5] M. Takeyama: Materials Science Forum, 3012 (2007) 539-543.
[6] D. Sholl, J.A. Steckel, Density functional theory: a practical introduction, John Wiley & Sons (2011) 17-25.
[7] K.P. Skokov, O. Gutfleisch: Scripta Materialia, 154 (2018) 289-294.
[8] W. Kohn, L.J. Sham: Physical review, 140 (1965) 1133-1138.
[9] J.P. Perdew, K. Burke, M. Ernzerhof: Phy rev letters, 77 (1996) 3865-3871.
[10] O.Y. Vekilova, B. Fayyazi, K.P. Skokov, O. Gutfleisch, C. Echevarria-Bonet, J.M. Barandiaron, A. Kovacs, J. Fischbacher, T. Schrefl, O. Eriksson: Phy Rev B, 99 (2019) 024421-024429.
[11] G. Kresse, D. Joubert: Phy Rev B, 59 (1999) 1758-1763.
[12] D.J. Chadi, M.L. Cohen: Phy Rev B, 8 (1973) 5747-5754.
[13] D. Goll, T. Gross, R. Loeffler, U. Pflanz, T. Vogel, A. Kopp, T Grubesa, G. Schneider Hard: Phy Sta Solidi RRL, 11 (2017) 1700184 (1-4).
[14] A.D. Boese, J.M. Martin, N.C. Handy: J of Chem Phys, 119 (2003) 3005-3014.
[15] A. Tanto, T. Chihi, M.A. Ghebouli, M. Reffas, M. Fatmi, B. Ghebouli: Resu in Phy 9 (2018) 763-770.
[16] F. Weber, L. Pintschovius, W. Reichardt, R. Heid, K.-P.Bohnen, A. Kreyssig, D. eznik, K. Hradil: Phy Rev B, 89 (2014) 10450 (1-13).
[17] M. D. Segall, P.J.D. Lindan, M.J. Probert, C.J. Pickard, P.J. Haspin, S.J. Clark, M.C. Payne: J of Phys Cond Matter, 14 (2002) 2717-2744.
[18] J.P. Perdew, S. Burke, M. Ernzerhof: Phys Rev Letters, 80 (4) (1998) 891–891.
[19] L. Fast, J M. Wills, B. Johansson and O. Eriksson: Phys Rev B, 51 (1995) 17431-17438.
[20] M. Born, K. Huang: Dynamical Theory of Crystal Lattices, Clarendon, Oxford, (1956) 120-124.
[21] Q.K. Hu, Q.H. Wu, Y.M. Ma, L.J. Zhang, Z.Y. Liu, J.L. He, H. Sun, H.T. Wang, Y.J. Tian: Phys Rev B, 73 (2006) 214116 (1-5).
[22] P. Ravindran, L. Fast, P. A. Korzhavyi, B. Johansson, J. Wills and O. Eriksson: J of Appl Phys, 84 (1998) 4891-4904.
[23] C.F. Cline, H.L. Dunegan, G.W. Henderson: J of Appl Phys, 38 (1967) 1944-1948.
[24] J. M. Leger, J. Haines, M. Schmidt, J.P. Petitet, A.S. Periera, J.A.H. Da Jornada: Nature, 383 (1996) 401.
[25] S.F. Pugh: Philos Mag, 45 (1954) 823-843.
[26] J. Haines, J.M. leger, G. Bocquillon: Ann Rev of Mater Res, 31 (2001) 1-23.
[27] O.L. Anderson: J Phys Chem of Sol, 24 (7) (1963) 909-917.
[28] R. Hill: Proc. Soc. London A, 65 (1952) 350.
[29] K. B. Panda and K. S. Ravi: Comput Mater Sci, 35 (2006) 134-150.
[30] C. Kittel: Introduction to Solid State Physics, 7th ed. Wiley, New York (1996) 15-21.